Genetic Programming and FEM simulation for a microscopic residual stress description in polycrystals using neutron diffraction and EBSD data

L Millán, G Carro-Sevillano, G Kronberger, O Garnica, I Collado, G Bokuchava, R Fernández, J I Hidalgo, P Halodova, A Sáez-Maderuelo, et al.

Genetic Programming and FEM simulation for a microscopic residual stress description in polycrystals using neutron diffraction and EBSD data

L. Millán[1]*, G. Carro-Sevillano[1], G. Kronberger[2], O. Garnica[3], I. Collado[1], G. Bokuchava[4], R. Fernández[1], J. I. Hidalgo[3], P. Halodova[5], A. Sáez-Maderuelo[6], and G. González-Doncel[1]

[1]*Department of Physical Metallurgy, Centro Nacional de Investigaciones Metalúrgicas (CENIM) C.S.I.C., Madrid E-28040, Spain*

[2]*Josef Ressel Center for Symbolic Regression, University of Applied Sciences Upper Austria, 4232 Hagenberg, Austria*

[3]*Adaptive and Bioinspired System Group, Universidad Complutense de Madrid, Madrid E-28040, Spain*

[4]*Frank Laboratory of Neutron Physics, Joint Institute for Nuclear Research, Dubna 141980, Russia*

[5]*Structural and System Diagnostic, Research Centre Rez, Prague 25068, Czech Republic*

[6]*Department of Technology, Centro de Investigaciones Energéticas, Medioambientales y Tecnológicas (CIEMAT), Madrid E-28040, Spain*

ABSTRACT

The detailed description of the residual stress fields in metallic polycrystals from the macro to the microscale is a problem of formidable complexity. This is mainly due to experimental limitations of diffractions tools and conventional analytical methods. Another key aspect that complicates the problem further is the possible generation of dislocation structures associated with the microscopic intergranular stresses in the polycrystal. This multi-scale nature of the dislocation structures and the present experimental and analytical limitations has suggested us to combine different tools to connect the residual stresses with the microstructure of the material at the different scales. In this work, Genetic Programming, GP, and finite element methods, FEM, simulations have been used to describe the intergranular residual stresses (those among individual grains) developed from a quenching step (axial component) in a polycrystalline 5083 aluminium alloy sample and their connection with the microstructure of the alloy. The computer tools make use of neutron diffraction and EBSD data as the experimental input information from the material´s microstructure.

Keywords: Residual Stresses; Genetic Programming; FEM; aluminium alloys, microstructure

---

* Corresponding author. *mglauri@cenim.csic.es*

1. Introduction

Metallic material components undergo in-service failure due, in many cases, to the presence of residual stresses, RS. It is known that the damage caused by these stresses manifests at different levels and in varying degrees of severity. The most worrying nowadays are microscopic stresses, m-RS, because they are generated at the microstructural scale, and their magnitude is not yet known. In particular, inter-granular stresses, those existing among neighboring grains, may be the origin of cracks across grain boundaries. These stresses are generated during material/component manufacture and ulterior thermo-mechanical processes. While the determination of RS fields at the macroscopic scale, M-RS, is somewhat overcome using analytical diffraction methods (direct use of Bragg´s law) and classical linear elasticity theory, undertaking this task at the microscopic level remains to be done.

Recent studies have attempted to quantify stresses at the grain level [1-3]. However, the invasive characteristics of the techniques used mean that the potential errors associated with the measurements remain high. Diffraction methods are, nowadays, the most powerful tool to investigate RS. The RS, specifically the M-RS, are determined from the displacement of the diffraction peaks obtained in the diffraction pattern; *i.e.*, peak shift from the relaxed position to the stressed one. However, it is known that RS, as a whole, also affect the peak shape, width, and maximum height. The problem relies in that the extraction of the specific stress held by individual grains from the information supplied by the diffraction peaks is, unlike the M-RS, of great complexity. In other words, the conventional analytical methods used for the M-RS cannot be used in this case. To achieve this purpose, a very detailed description of the microstructure, including parameters such as, grain morphology, size, close neighbors, crystal orientation, etc., seems to be needed; It is reasonable that the stress of individual grains is dependent not only on the thermomechanical process underwent by the material, but also on the surrounding grain microstructure. Using this information, together with that supplied by the diffraction experiments, seems a realistic starting point to address this problem.

In this work, Genetic Programming, GP, and simulations using the Finite Elements Method, FEM, are used to deepen into the RS state of individual grains in a single-phase aluminum alloy. The results obtained using both procedures are discussed to take further steps in the objective of quantifying these m-RS. On one hand, the use of Machine Learning, ML, tools, is here used to reproduce the diffraction peak profile generated by grains with a given *hkl*, and minimizing the error associated with the measurement. This approach is based on the use of Genetic Programming, GP, algorithms. These algorithms provide an expression which predicts the real peaks by “assigning” specific stress to specific grains. Of particular interest in this work is the sensitivity analysis of the possible microstructural parameters affecting the m-RS. On the other hand, FEM is used to analyze the RS developed in individual grains with different yield stress with respect the surrounding medium. The grains are appropriately located in the microstructure, at different locations with respect the sample central axis, and the resulting stress evaluated.

2. Materials and methodology

An extruded bar (40 mm in diameter) of aluminum alloy AA5083 was selected for this study. This single-phase alloy will yield more robust results due to its simple, non-ageing nature. In other words, the absence of a precipitation sequence, which would affect diffraction peak position and “distort” the calculation the stresses generated, facilitates the overall RS analysis; only thermo-mechanical treatments will be responsible of the RS state developed at the macro and microscopic scales. To simplify the problem as much as possible, a cylindrical sample, 60 mm in length and 25 mm in diameter, extracted from the center of the alloy bar, was used. The RS fields, at the macro and microscopic levels, were generated from a quenching treatment in fresh water after sample annealing at 530ºC during some 3 hours. From previous studies [4-5], it is known that the resulting profile of the M-RS field responds to a parabola, if observed from a longitudinal cross section of the sample (or a plane parallel to the extrusion axis, and passing through the center of the cylinder). The neutron diffraction experiments were conducted on the Fourier Stress Diffractometer, FSD, operating at the IBR-2 pulsed reactor in the Frank Laboratory of Neutron Physics, FLNP, of the Joint Institute for Nuclear Research, JINR,

(Dubna, Russia). The sample was, then, sectioned to extract small cube samples along the cross section of the cylinder (at the mid-height), to study the microstructure at the center of the sample (x=0) and the external region (x=12 mm), to account for the gradient resulting from the extrusion. Electron backscattering diffraction, EBSD, was used for this purpose. The specific details of the neutron diffraction and EBSD measurements are described elsewhere [6-7].

3. Genetic Programming

GP algorithms were designed with the aim of finding an expression of the lattice spacing, $\boldsymbol{d_i^{hkl}}$, that depends on microstructural parameters. These algorithms search among a set of initial expressions the one that best fit the real neutron diffraction peak. The algorithm assigns a $\boldsymbol{d_i^{hkl}}$ value to every grain within the range of lattice spacing values within the peak. A maximum number of generations, a crossover ratio and mutation probability of the expressions generated, as such as the limit on their length, have been established.

The microstructural parameters considered in this procedure are: grain area (size), number of near neighbors to each grain, their aspect ratio, and the slope of the long grain axis with respect the radial direction of the cylinder. Thirty runs were performed to validate the models**.** Resulting sensitivity analysis using the expressions predicted by GP is summarized in the plots of figure 1. For each microstructural parameter of the above ones, the mean of the other three was calculated and these values were kept fixed, varying only the one under study. The analysis indicates that the trends described by the predicted expressions appear to be a reflection of the mechanical behavior of the grains. Figure 1A, for example, shows the most influential parameter for *111* grains (the hardest ones) appears to be the Slope. This influence, even more pronounced and with a single trend, is maintained for the outer grains (figure 1C). This suggests that high values of the slope increases d_i^{hkl}, and therefore the stress. The two tendencies in the center may be attributed to grains of different nature within this group. On the other hand, while the lattice spacing decreases with the aspect ratio of grains in the center, it increases it in the outer grains. However, the number of neighbors does not seem to be relevant, as revealed by the high dispersion. The latter seems to be due to the nature of the surrounding neighboring grains. Finally, the Area does not seem to influence d_i^{hkl} in the center, but it does become important in the outer grains, minimizing their stress as Area increases.

In the case of the *200* grains (figure 1B and 1D), the influence of slope seems to decrease, although it shows again two behaviors. Aspect ratio is the least important parameter at the center, while area and number of neighbors, especially the latter, seem to be the most relevant. Again, the number of neighbors shows a greater dispersion and a negative trend, possibly since as this parameter increases, the probability that these are 200 (soft) or 311 grains (intermediate hardness) also increases, as these grains are the most abundant at this location. On the outside, it is observed that if the grains are deformed, the stresses are minimized according to the variations of the aspect ratio. It should not be forgotten that these grains are the softest, so it seems reasonable that they tend to modify their spherical shape to the constraints imposed by the environment. The number of neighbors is still relevant, while the area does not influence this position.

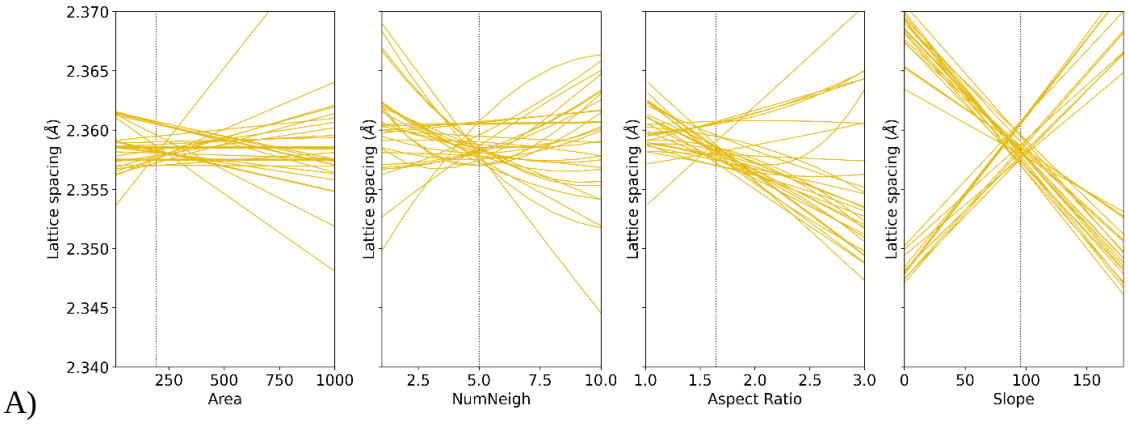

A)

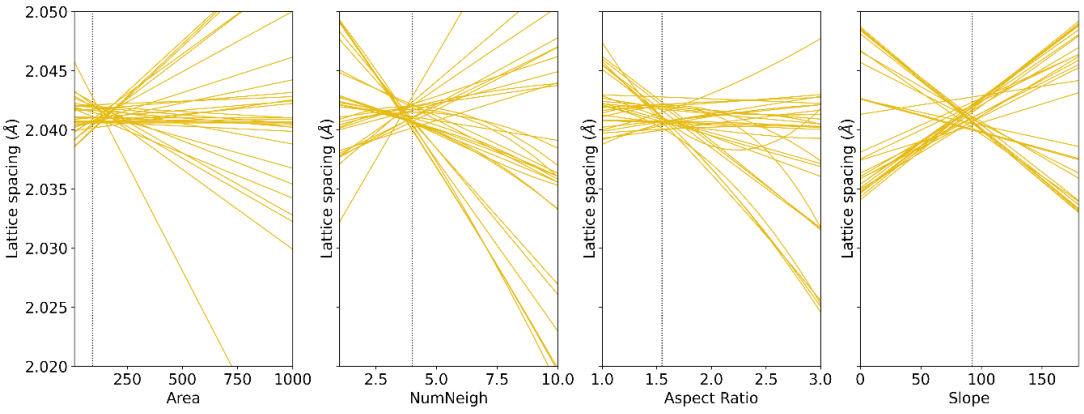

B)

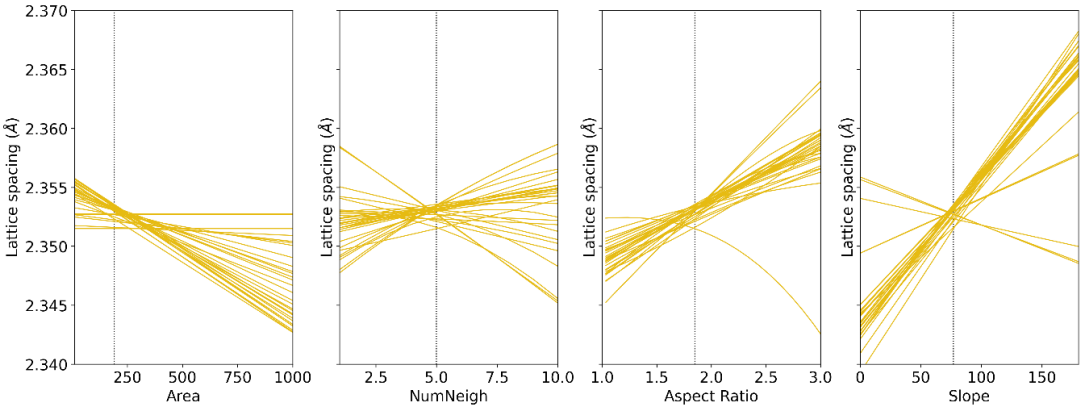

C)

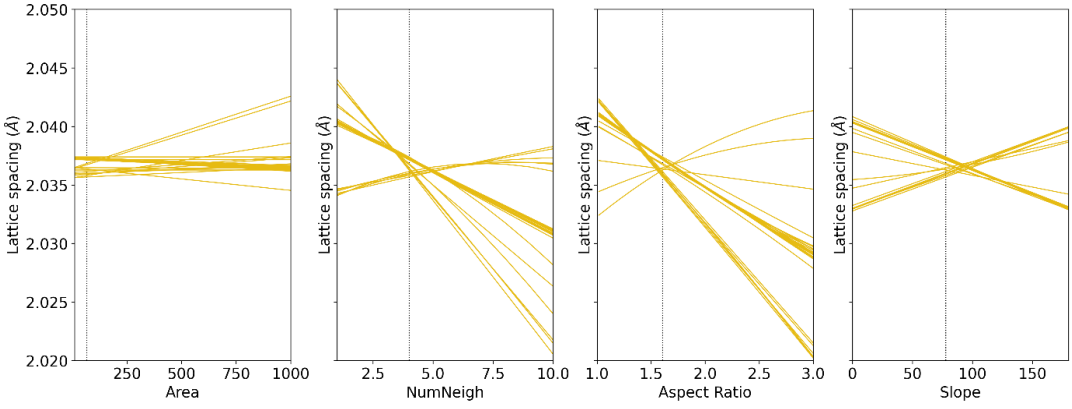

D)

Figure 1. Sensitivity analysis resulting from GP, after 30 runs. A) grains with 111 parallel to the extrusion axis, at x=0 mm (sample central region). B) grains with 200 parallel to the extrusion axis, at x=0 mm. C) grains with 111 parallel to the extrusion axis, at x=12 mm (sample outer region). D) grains with 200 parallel to the extrusion axis, at x=12 mm.

4. Finite element modelling.

The Heat Transfer, Nonlinear Structural Materials and Structural Mechanics Modules of COMSOL Multiphysics software were used to simulate, using FEM, the evolution of the RS during the quenching process. The simulation considers that the sample is fully submerged in the quenching media. The thermo-mechanical behavior is simulated using a directly coupled formulation. The heat conduction problem is solved independently from the stress problem to obtain temperature history. The formulation considers the contribution of the temperature field variation with time to the stress analysis through thermal contraction, as well as temperature-dependent thermal and mechanical properties. The solution is obtained from two steps. First, the temperature distribution and its history in the quenching model are computed by the heat conduction analysis. At this point, it is critical the heat transfer coefficient, HTC. The HTC evolution with temperature calculated according with [8] has been used. The convective heat flux, q, across the external surface of the cylinder is described as:

$$q = \mathrm{h} \cdot (T_{ext} - T) \qquad (1)$$

where h is the heat transfer coefficient and T_{ext} and T the temperature of the water reservoir and the cylinder, respectively. The temperature history is employed as a thermal load in the subsequent mechanical elastic–plastic calculation of the RS field. In this model, the length and radius of the cylinder and water reservoir are 60 mm by 12.5 mm (as the sample used in the experiments), and 400mm by 125mm, respectively, Figure 2.

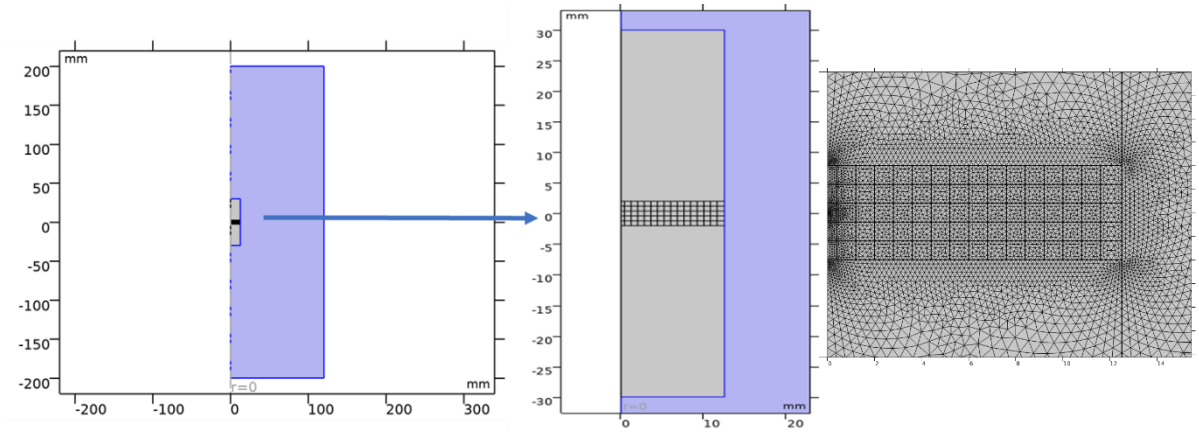

a) b) c)

Figure 2. Geometry of the FEM system showing a) real comparison between the cylinder and the water reservoir (blue) and b) detailed distribution of grains along radial direction and c) meshing elements used for the central part (mid-height) of the cylinder.

Because of the cylindrical symmetry, a 2D FEM is developed around the length axis of the cylinder. A triangular free mesh has been used, Fig. 2c), with 1216 edge elements and 112 vertex elements. The largest element is 4mm and the smallest one is 0.01mm. The grid is designed such that it gets finer close to grains squares. The external boundary of the cylinders is free. A square of 1x1mm^2 located at the (0,0) position is fixed during the quenching. This allows deformation of the sample and prevents from sample displacement during cooling.

4.1. Mechanical constitutive laws.

The mechanical model chosen to simulate the behavior of the material is based on previous work on RS development during quenching [6]. The aluminum cylinder has been modelled as an isotropic material. In the quenching process the temperature drops suddenly from 530ºC (803K) to room temperature. As the mechanical behavior of the material depends on the temperature, its response should vary from almost pure plastic behavior at high temperature to an elasto-plastic one at room temperature. This evolution was simulated with a thermo-elasto-

plastic constitutive model. The plastic behavior is defined as thermal softening; *i.e.* temperature dependence of yield strength and isotropic hardening. The definition of temperature dependent material properties (the elastic limit among them) allows a gradual increase of the residual stress field (Von Misses) as the temperature decreases. The total strain tensor, ε, is the driven variable of the mechanical problem computed in terms of the displacement field, *u*, as:

$$\epsilon = \frac{1}{2}\left[(\nabla \mathbf{u})^{\mathsf{T}} + \nabla \mathbf{u} + (\nabla \mathbf{u})^{\mathsf{T}} \nabla \mathbf{u}\right] \tag{2}$$

The constitutive model including stress equilibrium can be written as:

$$\begin{aligned} &\underbrace{0 = \nabla \cdot (\mathsf{F}\,\mathsf{S})^{\mathsf{T}} + \mathbf{F}_{\mathsf{V}}}, \quad \mathsf{F} = \mathsf{I} + \nabla \mathbf{u} \\ &\mathsf{S} = \mathsf{S}_{\mathsf{ad}} + J_{\mathsf{i}} \mathsf{F}_{\mathsf{inel}}^{-1} \left(\underbrace{\mathbf{C} : \varepsilon_{\mathsf{el}}} + \left(-\frac{1}{3} \mathrm{trace}(\mathbf{C} : \varepsilon_{\mathsf{el}}) - p_w \right) \mathsf{I} \right) \mathsf{F}_{\mathsf{inel}}^{-\mathsf{T}}, \quad \varepsilon_{\mathsf{el}} = \frac{1}{2}\left(\mathsf{F}_{\mathsf{el}}^{\mathsf{T}} \mathsf{F}_{\mathsf{el}} - \mathsf{I} \right), \quad \mathsf{F}_{\mathsf{el}} = \mathsf{F}\mathsf{F}_{\mathsf{inel}}^{-1} \\ &\mathsf{S}_{\mathsf{ad}} = \mathsf{S}_0 + \mathsf{S}_{\mathsf{ext}} + \mathsf{S}_{\mathsf{q}} \\ &\mathbf{C} = \mathbf{C}(E, \nu) \end{aligned} \tag{3}$$

where the force, F, is expressed as the as the Second Piola-Kirchoff stress *S*, *E* is the (temperature dependent) elastic modulus and ν is the Poisson´s coefficient [9]. The thermal deformation is computed to the thermal contraction during the cooling process from 803K to room temperature. The plastic strain was described by a yield stress and a power-law hardening function with exponent 0.5.

4.2. Micro residual stress analysis by FEM.

FEM has been also used to describe the influence of some microstructural parameters on the m-RS generated from the quenching. Among the possible ones, the following parameters are considered here: grain size, aspect ratio, number of neighbors, slope, and texture. In particular, the results concerning the effect of texture and grain position on the intergranular stresses are presented. The present work does not intend to carry out an exhaustive study on the influence of microstructural parameters on the residual stress state. The aim is to show that the use of a combined GP and FEM strategy is effective in unravelling the highly complex correlation between microstructure and the m-RS field.

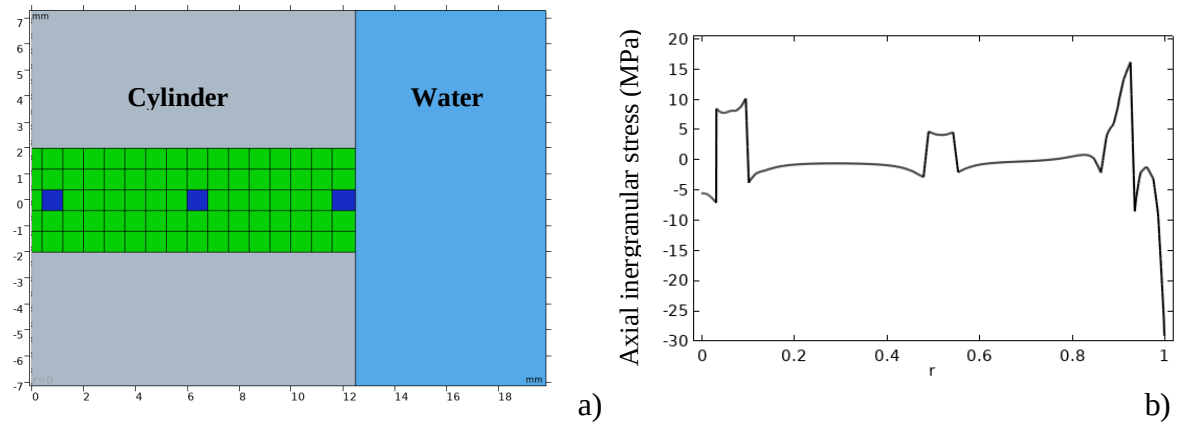

Figure 3. a) Distribution of high yield stress grains along sample dimeter and b) axial intergranular stress profile along sample radial direction.

First, a microstructure composed by three grains with a high yield strength located along the radial direction of the cylinder (figure 3a) is considered. The rest of the material is considered as a continuous medium. The yield strength of the blue grains is 25% higher than that of the polycrystal (average value). Figure 3b) shows the axial component of the m-RS between blue grains and those with the average value. The m-RS values obtained are small, < 45MPa. This result is not relevant, because the absolute values are not representative of the microscopic stress

state as the microstructure used in this case is not real. In fact, the cylindrical symmetry used in this FEM study provides sound conclusions of the axial and radial components. However, these results anticipate relevant information when the relative value of these m-RS at different positions along the radial direction of the sample are compared. In particular, the high yield strength grains located close to the symmetry axis or close to the outer surface, present a considerably higher stress value than those located at positions around r=6mm. In particular, the m-RS at the outermost position is at least three times higher that of the inner ones. This result shows that the quenching is more aggressive on the surface in contact with the medium, resulting in high m-RS.

In the following, a microstructure closer to the real one is considered, although it is still a simplified one (figure 4a). Specifically, the microstructures represented by the EBSD maps of figure 4 have been divided into grids of 5x5 elements. Each of these grid elements has been identified with the population of grains showing the highest volume fraction in this grid. Thus, there is a prevalence of high yield strength, blue grains, in the inner and outer zones of the cylinder, and average grains in the middle (figure 4a). The average grains have the same mechanical properties as the rest of the material, which is considered as a continuous medium. The blue grains in figure 4b) have, then, a yield strength 25% higher than the average and the red ones 25% lower. In this case, it is also observed that the intergranular stresses are strongly dependent on the position in which the grains are located. Figure 4c) shows the axial component of the m-RS among grains with high, low, and average yield strength. The m-RS are small, < 30MPa. As in figure 4b) the relevance of the results revealed in figure 4c), however, is related with the stress achieved at different positions along the radial direction. In particular, the grains with a high yield strength located close to the symmetry axis, present a considerably higher m-RS than in the central position. This result shows that, although the hardening aggressiveness near the symmetry axis of the specimen is low, high stresses develop if certain spatial arrangements of grains of different yield strength are present.

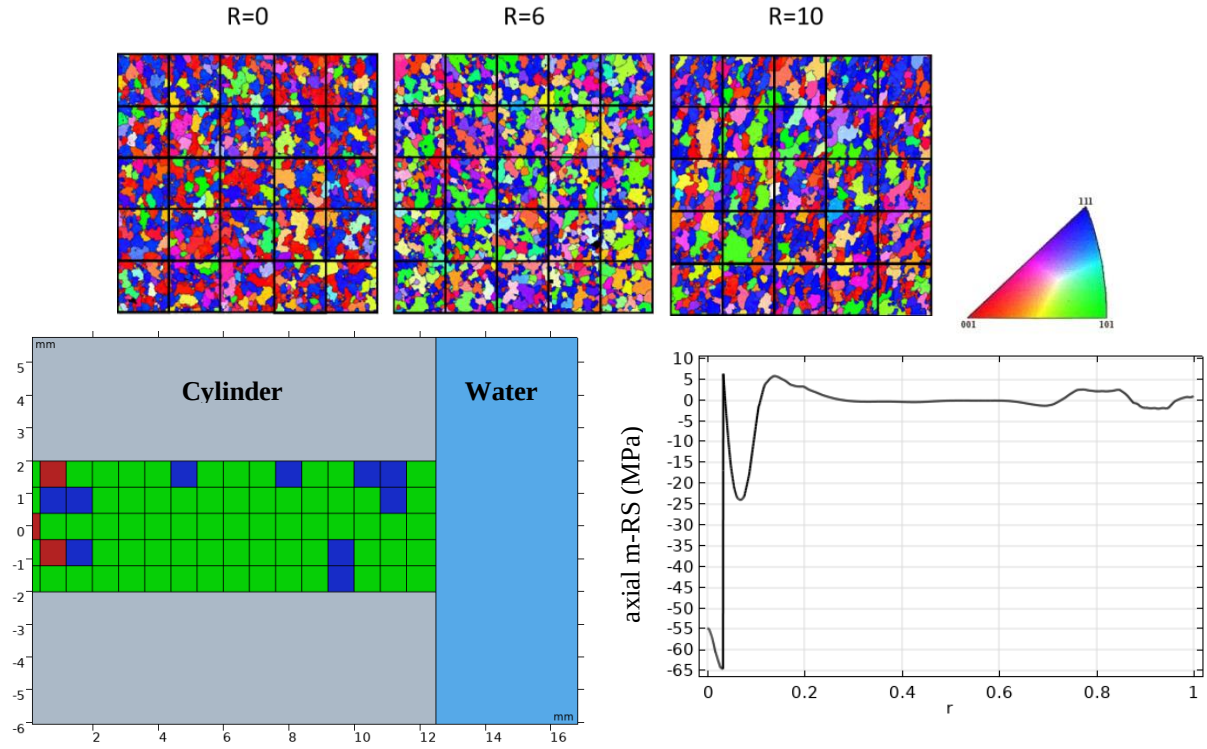

Figure 4. a) 5x5 grid over the real microstructure of the material investigated b) distribution of the high yield stress grains along sample radial direction, inverse pole figure, IPF, coloring reference for the extrusion axis and b) axial intergranular stress profile along radial direction.

Conclusions

The analysis of RS at a microstructural scale, m-RS, is a problem of extraordinary complexity. Even in very simplified cases, with good control of the thermomechanical process and the simplicity and high symmetry of the microstructure selected for the study, severe approximations are still needed to delve into the stress developed in individual grains. The m-RS depends not only on the specific characteristics (parameters) of the grains and the thermomechanical process undergone by the component, but also on the specific location of the grain in the component and the parameters of the surrounding neighbors. Techniques such as GP and FEM are used here to investigate these m-RS. The combination of both tools, together with microstructural data of the material, is revealed as an appropriate strategy to achieve this goal, although there is still a long way to go to achieve it.

Acknowledgements

This work has been supported by Spanish This work has been supported by Madrid Regional Goverment-FEDER grants Y2018/NMT-4668 (Micro-Stress-MAP-CM), MAT2017-83825-C4-1-R and B2017/BMD3773 (GenObIA-CM). Thanks also to the FLNR-JINP for the beam time allocated on FSD instrument, and the support by the Christian Doppler Research Association within the Josef Ressel Center for Symbolic Regression.

References

[1] Everaerts, J., Song, X., Nagarajan, B., & Korsunsky, A. M. (2018). Evaluation of macro-and microscopic residual stresses in laser shock-peened titanium alloy by FIB-DIC ring-core milling with different core diameters. Surface and Coatings Technology, 349, 719-724.
[2] Salvati, E., & Korsunsky, A. M. (2017). An analysis of macro-and micro-scale residual stresses of Type I, II and III using FIB-DIC micro-ring-core milling and crystal plasticity FE modelling. International Journal of Plasticity, 98, 123-138.
[3] Kumagai, M., Curd, M. E., Soyama, H., Ungár, T., Ribárik, G., & Withers, P. J. (2021). Depth-profiling of residual stress and microstructure for austenitic stainless steel surface treated by cavitation, shot and laser peening. Materials Science and Engineering: A, 813, 141037.
[4] Fernández, R., Ferreira-Barragáns, S., Ibáñez, J., & González-Doncel, G. (2018). A multi-scale analysis of the residual stresses developed in a single-phase alloy cylinder after quenching. Materials & Design, 137, 117-127. W. Strunk Jr., E.B. White, The Elements of Style, fourth ed., Longman, New York, 2000.
[5] Millán, L., Bokuchava, G., Fernández, R., Papushkin, I., & González-Doncel, G. (2021). Further insights on the stress equilibrium method to investigate macroscopic residual stress fields: Case of aluminum alloys cylinders. Journal of Alloys and Compounds, 861, 158506.
[6] Millán, L., Bokuchava, G., Hidalgo, J. I., Fernández, R., Kronberger, G., Halodova, P. & González-Doncel, G. (2021). Study of Microscopic Residual Stresses in an Extruded Aluminium Alloy Sample after Thermal Treatment. Journal of Surface Investigation: X-ray, Synchrotron and Neutron Techniques, 15(4), 763-767.
[7] Millán, L., Kronberger, G., Hidalgo, J. I., Fernández, R., Garnica, O., & González-Doncel, G. (2021, April). Estimation of Grain-Level Residual Stresses in a Quenched Cylindrical Sample of Aluminum Alloy AA5083 Using Genetic Programming. In International Conference on the Applications of Evolutionary Computation (Part of EvoStar) (pp. 421-436). Springer, Cham.
[8] N. P. H. Chobaut, Measurements and modelling of residual stresses during quenching of thick heat treatable aluminium components in relation to their precipitation state, École Polytechnique Fédérale de Lausanne: Thesis, 2015.
[9] HailongChen, «Constructing continuum-like measures based on a nonlocal lattice particle model: Deformation gradient, strain and stress tensors,» International Journal of Solids and Structures, vol. 169, pp. 177-186, 2019.